sustainability

MDPI

Article

Radon Hazard of the Zhurinsky Fault for the Population in the Kuznetsk Coal Basin: Primary Results

Timofey Leshukov [1,*], Konstantin Legoshchin [1] and Aleksey Larionov [2]

[1] Department of Geology and Geography, Institute of Biology, Ecology and Natural Resources, Kemerovo State University, 6 Krasnaya Street, 650000 Kemerovo, Russia; geology@kemsu.ru
[2] Department of Genetics and Fundamental Medicine, Institute of Biology, Ecology and Natural Resources, Kemerovo State University, 6 Krasnaya Street, 650000 Kemerovo, Russia; larionov@kemsu.ru
* Correspondence: tvleshukov@kemsu.ru

Abstract: The aim of this study is the primary assessment of radon hazard of the Zhurinsky fault of the Kuznetsk coal basin, in the territory of the Salair–Altai–Irtysh fold. Soil radon content, radon flux densities, their spatial characteristics and correlations with each other and with other factors were evaluated. We found that soil radon concentration varies within the range of 3599 to 14,413 Bq/m^3 (mean value 8766 ± 569.8 Bq/m^3), and radon flux density ranges from 23 to 147 mBq·m^{-2}·s^{-1} with a mean value of 67.19 ± 1.31 mBq·m^{-2}·s^{-1}. A correlation with air temperature, pressure and humidity was found, which decreases with the depth of the measurements. All studied parameters in space are clustered ($p \leq 0.1$). At the same time, the whole studied area in the vicinity of the tectonic disturbance should be classified as radon-hazardous, and residential structures located within its boundaries as potentially hazardous. Our study contributes to understanding the radon hazard of crustal faults.

Keywords: radon flux density measuring; soil radon measuring; tectonic faults; radon exhalation; Kuznetsk coal basin

check for updates

Citation: Leshukov, T.; Legoshchin, K.; Larionov, A. Radon Hazard of the Zhurinsky Fault for the Population in the Kuznetsk Coal Basin: Primary Results. *Sustainability* **2023**, *15*, 16774. https://doi.org/10.3390/su152416774

Academic Editor: Francesco Faccini

Received: 22 October 2023
Revised: 6 December 2023
Accepted: 11 December 2023
Published: 12 December 2023

Copyright: © 2023 by the authors. Licensee MDPI, Basel, Switzerland. This article is an open access article distributed under the terms and conditions of the Creative Commons Attribution (CC BY) license (https://creativecommons.org/licenses/by/4.0/).

1. Introduction

Radon is a noble radioactive gas that is a sufficient threat to public health. The most significant radon isotopes are Radon (^{222}Rn), Thorone (^{220}Rn) and Actinon (^{219}Rn). Because of its longer half-life (T1/2 = 3.82 days) ^{222}Rn is more abundant than other isotopes. It has the ability to migrate and accumulate in soil air and indoors including residential buildings [1,2].

Residential radon exposure is up to 50% of the average annual exposure by ionizing radiation for the human population, this causes a significant health risk especially in areas with excessive radon levels [3]. Lung cancer is considered the main health effect of long-term radon exposure [4–8].

Many researches aimed to evaluate the geogenic radon level, and its essential connection with tectonic disturbances was noted [9–13]. The upper part of the earth's crust can be classified as fissure-pore geological objects. Radon is released from rocks into pores and crevices. Territories where tectonic disturbances were discovered are characterized by a large volume of fissure-pore space in the geological environment, which contributes to the accumulation of significant amounts of radon. Radon is subsequently transferred from these voids to the surface through diffusion, convection and other forces. Associated gases, especially methane and hydrogen, are satellite gases that act as vehicles for radon migration. A change in the stress–strain state of rocks in the upper part of the earth's crust leads to significant changes in the volume of the pore–crack space. In the compression zone of the earth's crust blocks, a decrease in volume occurs. Consequently, this results in a low volume of radon and the low ability to move to the surface along the fault zone. In the stretch zone, there is an increase in the space for underground gases. Active faults tend to show significant temporary changes in the radon field above them, while inactive faults

tend to be more stable or not expressed at all [2,14–17]. Faults are a permeable environment for ground water, fluids and gases [18,19]. Their permeability depends on the type of fault (thrust, shear, etc.) [20,21], the minerals filling the fractures and their composition features [22], the tectonic activity of the faults, meteorological parameters, etc. [17,23]. It is currently assumed that faults act as transport channels for radon which is released from rocks and accumulates in significant amounts in the cavities in Earth's crust [2,14–16]. This fact constitutes the basis for the widely used methodology of fault identification by radon measurement data [24,25]. Previous research demonstrated that above fault zones, areas of significant concentrations of soil radon are formed, from which it emanates to the surface. Such high radon areas with can significantly exceed the surface areas of the rock crushing zones which accompany tectonic disturbances [20]. Active faults can be identified by high soil radon content and its emanations to the surface. In some cases, fault zones, in the absence of modern geodynamic processes, become non-permeable due to the filling of cracks with secondary carbonate, siliceous and other minerals. Also, the radonometric survey of faults allows for the prediction of earthquakes and rock and tectonic shocks during engineering and geological explorations [17,26–28].

The assessment of the radon-associated hazard of tectonic disturbances becomes more valuable in areas of intensive mining activity. The Kuznetsky coal basin is the oldest coal mining region in Russia with a high degree of urbanization, population density and the deep mineral mining specialization of the economies of most cities. A significant part of the territory of coal-mining towns was affected by underground coal mining, which led to the formation of areas of high radon emission risk. In previous research in the mined area, we found a significant increase in radon emanation to the surface and its volume activity indoors [29,30]. Similar patterns have been observed in coal mining areas in Poland, Germany, UK, Russia, China and other countries [31–36]. Recently, residential structure construction is not permitted within mining areas in Russia. Therefore, the assessment of tectonic faults is necessary because they are the natural boundaries of mines and often, the only suitable areas for new residential building replacement in mining-associated towns are the areas above these faults.

Residential buildings located on soils with a substantial concentration of radon in the underground atmosphere or high emanation to the surface pose a significant threat to public health. The release of radon into living spaces from the soil is due to the "pump effect" that relies on a temperature difference [37,38]. High levels of radon in the soil resulting from faults in the Earth's crust may increase the cancer risk for inhabitants of the Kuznetsk coal basin. The Zhurinsky fault crosses a rather large residential area of the Kuznetsk coal basin. About 7500 residential buildings are located at a distance of 500 m in each direction from the displacement, mostly from Leninsk-Kuznetsky, Polysaevo, Promyschlennaya and some settlements of the Belovsky district. If a wider influence of the lithosphere on the radon field is detected at this fault zone, the number of potentially affected buildings may increase significantly.

Aim: to assess the radon hazard of the Paleozoic tectonic fault—the Zhurinsky fault. In addition, the Salair and southern parts of the Kuznetsk coal basin have a block geological structure. The boundaries of the blocks are tectonic disturbances similar to the Zhurinsky fault. They are syngenetic, similar in dynamics and type to the Zhurinsky fault, and were formed in the same folding era. By studying the radon hazard of the Zhurinsky fault, we obtain important information about the permeability of faults of this type in Kuzbass.

2. Materials and Methods

2.1. Study Location

The study area is located in the Kuznetsk coal basin, within the Salairo-Altai-Irtysh folded area belonging to the Hercynian folding epoch. The main tectonic disturbances completed their development during this epoch, but some of them were rejuvenated during the Neogene-Quaternary. The soils of the study area are represented by leached chernozem. The relief altitude difference is 5 m, the average height above sea level is 220 m.

Figure 1 shows the study area, the location of the observation points and the area of distribution of this fault in the Kuznetsk Trough.

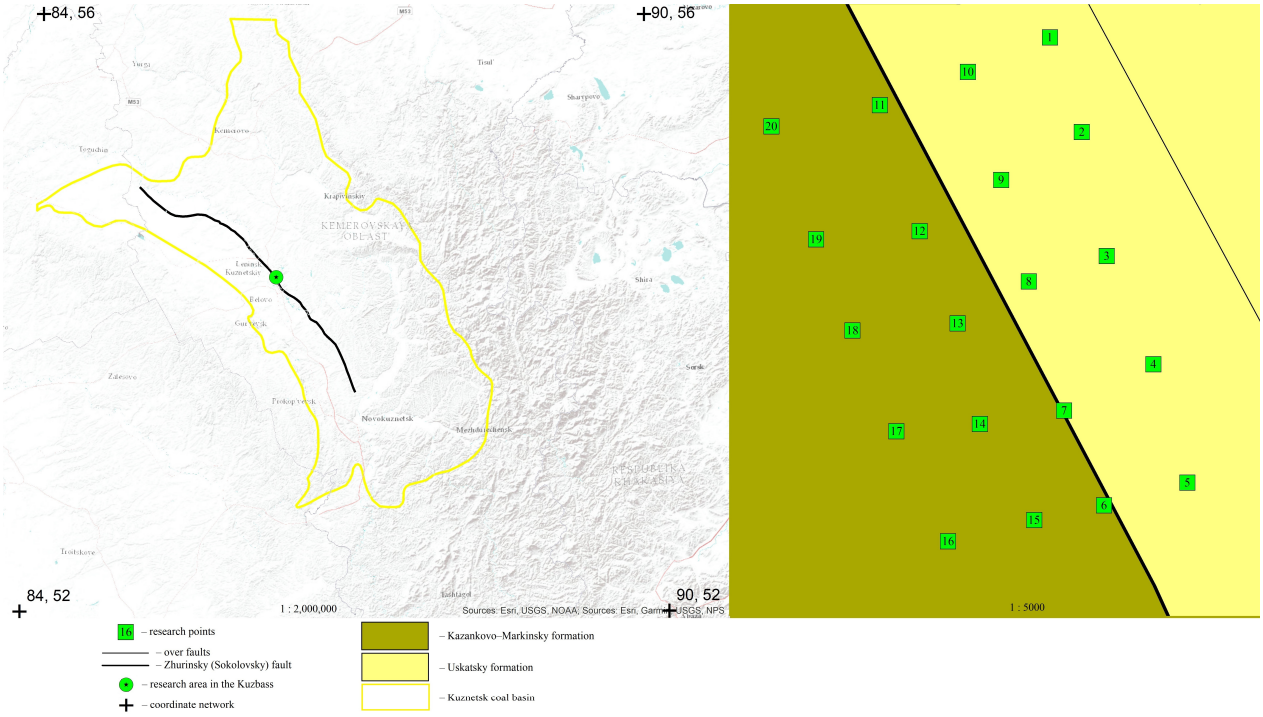


Figure 1. Investigation area.

Geologically, the study area is represented by two tectonic blocks separated by the Zhurinsky fault. The blocks are composed of rocks of the upper Permian system and belong to the Uskatsky and Kazankovo–Markinsky formations. The formations are represented by the rhythmic interlacing of sandstones, siltstones and coals, with subordinate mudstones. Paleozoic rocks are crushed into brachysynclinal folds. Anticlinal folds are of subordinate importance, most often large interblock faults are laid along their cores, an example of which is the Zhurinsky fault. The Permian sediments are overlain by the Cretaceous-Paleogene weathering crust and Cenozoic N-Q sediments. The thickness of Q sediments is 35–50 m. The lower part of the Eopleistocene sediments, the Sagarlyk Formation, lies below. It is overlain by the Kedrovskaya Formation of the Lower-Middle Pleistocene. The deposits of the 3rd supra floodplain terrace of the Upper Pleistocene are located further. All these sediments are alluvial deposits and are composed of clays and loams. The upper part of the section is represented by subaerial deposits (loess-like loams) of the Upper Pleistocene [39].

The Zhurinsky fault, along the strike, changes the angle and azimuth of the displacement dip. The fault itself developed as a convergent boundary of blocks and is related to strike-slip and thrusting in some places. This fault corresponds to a significant zone of rock crushing, mainly confined to the hanging wall. In the foot wall, the rocks are practically not dislocated and have small dip angles. The thickness of the crushing zone established during prospecting works is up to 300 m [40].

2.2. Soil Air Radon Volume Activity (VAR) and Radon Flux Density (RFD) Measurement

A total of 20 radon measurement points located within and outside the crushing zone belonging to the Zhurinsky fault zone were selected to study soil radon concentration and RFD (Figure 1). The measurement points were spaced 130–190 m apart in nearly orthogonal placement pattern. The general scheme of radon research at each point is presented in Figure 2.

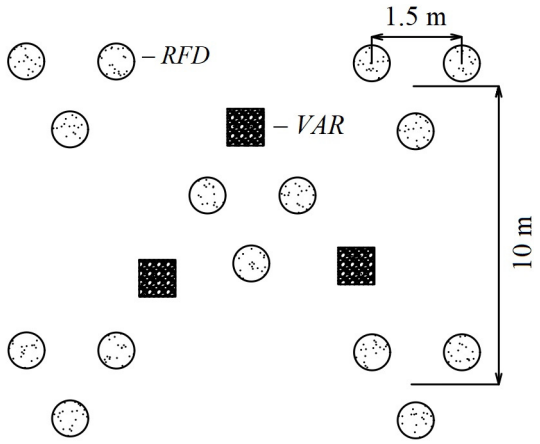


Figure 2. The general scheme of radon research at each point.

To measure RFD, 20 wells were drilled with a depth of 0.6 m and a diameter of 0.08 m. After the drilling was completed and before the measurements were taken, the wells were tightly covered with polyethylene and kept that way for at least 12 h. The Alpharad + radon monitor (NTM-Zashchita, Moscow, Russia) was used to measure soil radon. This monitor has a basic measurement uncertainty of ± 30%. Soil air was pumped into plastic tubes by an AV-07 air sampler (NTM-Zashchita, Moscow, Russia). The averaging of the radon content value was achieved by a long process of pumping air for 5 min through a closed system between the well and the container. The volumetric pumping speed of the air sampler is 1 ± 0.2 L/min. Further sample tubes were connected to the radon monitor collecting chamber and air was circulated for 5 min, then VAR measurements were performed for 20 min. After each measurement, the air probe intake and radon monitor chamber system was ventilated with atmospheric air for 5 min.

RFD was measured by a Camera-01 device (NTC-NITON, Moscow, Russia). This instrument has a basic measurement uncertainty of ±30%. This instrument evaluates radon activity by measuring the gamma- and beta-radiation of the short-lived radon progeny—^{214}Pb, ^{214}Bi, which are in equilibrium with radon. To achieve the equilibrium state of radon and its DPR, the selected sample was incubated for 4 h after the end of exposure. Exposure was performed using carbon sorption columns (SK-13) and an accumulation chamber (NK-32) (Figure 3).



Figure 3. Accumulation chamber for soil radon.

A total of 300 RFD measurements were made at 20 observation points. The collecting chambers were pressed firmly into the loose soil. Fifteen cameras (NK-32) per envelope were installed for each observation point. Next, the data from 15 measurements were averaged for each observation point to estimate the spatial variation of the RFD. The carbon sorption columns needed to be tightly closed, since radon can be desorbed from them into the atmosphere [41].

For all measurements, an internal measurement control was performed. Repeated measurements were 10–15% of previously performed measurements. The obtained values were within the limits of the method measurement errors declared by the manufacturer.

2.3. Statistical Analysis

Statistical processing of the data was performed using the Statistica 14.0 package (StatSoft, Tulsa, OK, USA). Distribution verification was carried out using Kolmogorov–Smirnov, Liliefors, Shapiro–Wilk tests. Statistical significance was accepted at the level of $p \leq 0.05$. Correlation analysis between RFD, soil radon VAR and weather conditions was carried out using the Pearson correlation coefficient. Statistical significance was accepted at the level of $p \leq 0.05$.

2.4. Spatial Methods

All spatial research methods were performed using the ArcGIS 10.8.1. program. To find out the spatial covariance of the data, we used Moran's I method, with a statistical significance $p \leq 0.1$. Also, the NaturalNeighbor tool in ArcGIS 10.8.1 was used for the interpolation of soil radon and RFD.

2.5. Meteorological Conditions during Research

Soil air VAR and RFD were measured without significant rainfall (no more than 0.01 mm per day). Soil air VAR measurements were made over 4 days. Air temperature ranged from 13 °C to 20 °C, with a mean of 16.1 ± 0.51 °C. Pressure varied from 983.5 hPa to 987.3 hPa with a mean value of 985.8 ± 0.26 hPa. Humidity ranged from 46% to 77% with a mean of 62.05 ± 2.2%.

RFD was measured over 2 working days. The air temperature during sorption column exposure ranged from 15.33 °C to 17.17 °C, with a mean value of 16.43 ± 0.13 °C. The pressure varied from 984.5 hPa to 986.2 hPa with a mean value of 985.4 ± 0.14 hPa. Air humidity varied from 52.92% to 61.78% with a mean value of 57.26 ± 0.83%.

The temperature, pressure and humidity were acceptable for measurements according to the method, with an error not exceeding 30%.

3. Results

3.1. Soil Air VAR

The soil air VAR varied from 3599 to 14,413 Bq/m^3 (mean value 8766 ± 569.8 Bq/m^3, median value 9246.3 Bq/m^3 (Table 1). The distribution of this value is fitted to normal distribution ($p \leq 0.05$).

No correlation was found between soil VAR and the distance (from 5 to 378 m, with mean value 206 m) of the observation point from the Zhurinsky fault displacement (r = 0.28, $p > 0.05$).

A correlation of moderate strength was found between soil radon content and air temperature (r = 0.45, $p \leq 0.05$). Additionally, an increase in correlation was noted between mean air temperature one hour before observations and soil radon content (r = 0.50, $p \leq 0.02$), as well as two hours (r = 0.52, $p \leq 0.02$) and three hours (r = 0.53, $p \leq 0.02$) later.

Table 1. Descriptive analysis of soil air VAR.

N°	Soil Radon VAR, Bq/m^3	SE, Bq/m^3	Distance to Fault, m
1	9302	2790	383
2	9244	2772	346
3	5689	1706	262
4	6809	2043	240
5	9579	2873	181
6	9248	2774	16
7	10,354	3106	5
8	5791	1737	73
9	7410	2223	127
10	3599	1079	176
11	9731	2919	42
12	8062	2418	98
13	5744	1723	120
14	12,535	3760	184
15	10,523	3157	177
16	14,413	4324	378
17	12,740	3821	365
18	9890	2967	345
19	8915	2674	321
20	6774	2032	290
All	8766	596.8	206

3.2. RFD

Table 2 represents the descriptive statistics of RFD.

Table 2. Descriptive analysis of RFD.

Research Point	Radon Statistics, mBq·m^{-2}·s^{-1}							Distance to Fault, m
	RFD	SE	Median	Max	Min	Interval	Percent over 80	
1	59.67	3.98	58	77	31	46	0.0	383
2	48.93	3.68	47	80	23	57	6.7	346
3	67.13	6.67	68	120	30	90	26.7	262
4	59.33	4.05	60	91	36	55	13.3	240
5	51.07	5.93	45	107	25	82	6.7	181
6	52.60	5.30	57	88	24	64	6.7	16
7	53.27	4.18	50	84	30	54	6.7	5
8	51.27	2.54	51	66	37	29	0.0	73
9	45.13	2.46	44	60	31	29	0.0	127
10	55.93	3.31	55	81	37	44	6.7	176
11	73.27	5.26	75	104	28	76	40.0	42
12	90.33	6.58	96	147	57	90	53.3	98
13	93.67	4.39	97	122	71	51	66.7	120
14	84.00	5.37	83	129	54	75	53.3	184
15	77.07	4.11	81	100	46	54	53.3	177
16	78.93	6.53	71	124	49	75	40.0	378
17	76.20	4.76	70	111	58	53	33.3	365
18	71.20	4.08	71	109	44	65	26.7	345
19	78.33	2.87	78	97	61	36	40.0	321
20	76.40	4.96	70	115	54	61	33.3	290
All	67.19	1.31	65.5	147	23	124	45.0	206

The RFD ranged from 147 to 23 mBq·m^{-2}·s^{-1} with a mean value of 67.19 ± 1.31 mBq·m^{-2}·s^{-1}. The median value is 65.5 mBq·m^{-2}·s^{-1}, and this distribution fits the normal one. In the study area, there were three monitoring sites with a mean value above 80 mBq·m^{-2}·s^{-1}, which according to the radiation protection standards (NRB-99/2009) [42] in residential buildings, requires a moderate form of building protection against geological radon.

In 17 monitoring sites, values above 80 mBq·m^{-2}·s^{-1} were also found. The proportion of the obtained values of RFD above 80 mBq·m^{-2}·s^{-1} is 45% of all observations (300 measurements) and from 0 to 66.7% of all measured values within each observation point.

No correlation was discovered between the distance of the observation point from the Zhurinsky fault displacement and RFD (r = 0.16, $p > 0.05$). Also, we did not find a relationship between soil VAR and RFD (r = 0.24, $p > 0.05$). We found a correlation between RFD and mean air temperature (r = 0.89, $p \leq 0.01$), air pressure (r = −0.84, $p \leq 0.01$) andair humidity (r = −0.90, $p \leq 0.01$) at the moment of the exposure of the storage chambers.

3.3. Spatial Patterns of RFD and Soil Air VAR

Table 3 displays the spatial Moran's I autocorrelation data.

Table 3. Descriptive analysis of Moran's I.

	Soil Air VAR	RFD
Observed	0.300598	0.398172
Expected	−0.052632	−0.052632
Standard Deviation	0.037165	0.039221
z-score	1.832277	2.276297
p-value	0.066910	0.022828

In both cases, the null hypothesis of chaotic data distribution is unlikely—for soil radon $p \leq 0.07$, for RFD $p \leq 0.02$. High Z-score values indicate data clustering. High values are clustered in the hanging wall of the fault. Figure 4 presents the spatial characteristics of soil radon VAR and RFD changes.

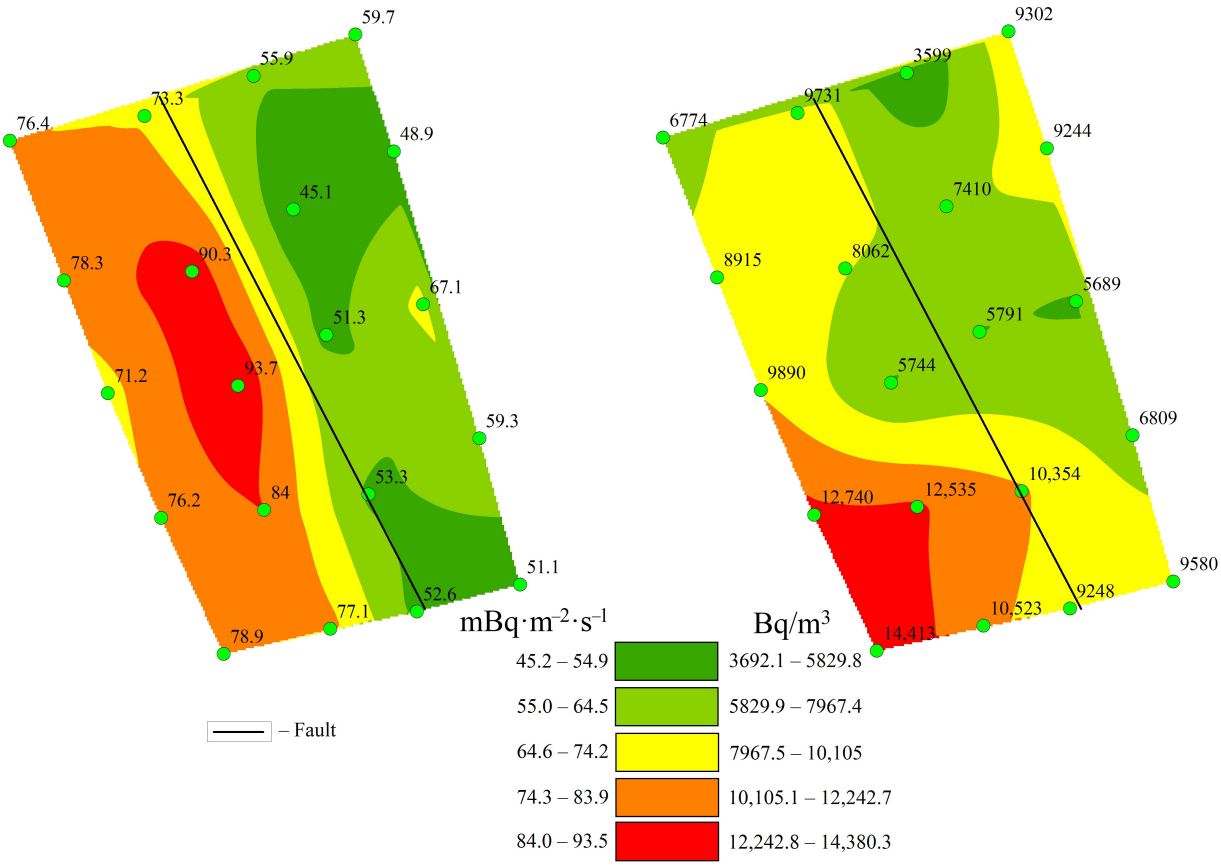


Figure 4. Spatial features VAR and RFD.

4. Discussion

4.1. Soil Air VAR

High soil VAR indicates the presence of a radon permeable medium. To assume its removal from deep soil horizons is currently not possible, as additional studies on hydrogen content are required, similar to this research [23]. Increased radon volume activity suggests a high potential for radon migration to residential buildings located above and near this fault area. Previously, we found buildings with high radon concentrations located near this fault zone. Within 1 km from the disturbance, the average VAR in the studied houses was 331.9 Bq/m^3, within 500 m–271.5 Bq/m^3, within 200 m–218 Bq/m^3 [29,30]. A similar relationship between soil radon and residential building VAR was also observed in Italy [43]. High values of soil VAR can be caused by the local geological situation—the content of parent elements (Ra, U), moisture, soil porosity or permeability caused by tectonic disturbances. Also, the growth of soil radon concentrations in the area of faults can be stimulated by methane and carbon dioxide venting to the surface which, as noted above, can stimulate radon migration through permeable zones [44–46]. It is known that in coal-bearing strata, the content of methane and carbon dioxide will be quite high. It is also known that coal and coal-bearing rocks can contain high concentrations of uranium and radium [47]. Also, the type of crushing zone could influence the formation of such a large area with high values. Radon from a disturbance can be localized along the line of the displacement or it may not be detected in the displacement at all, and other options are also possible [48]. However, according to Swedish criteria [49], values above 10,000 require conventional measures to reduce the entry of radon into residential premises. In our work these are 4 observation points. But with depth, the situation can change significantly [50].

The lack of correlation between the distance from the displacement site and the soil radon content can be explained by this distance being insufficient to observe the impact of faulting on soil radon content. The variation in soil radon values can be attributed to local characteristics (composition of loose sediments, radium content, etc.). Furthermore, our observations did not extend beyond the influence of the fault and its associated fracture zone. Previously, in a study of soil radon and its emanation in a fault zone, it was found that the composition of gas in the soil changes and increases over a larger area than the crushing zone of the fault [20,21]. This was also observed for residential buildings, where an increase in VAR is observed as they near the fault zone [43].

The moderately strong correlation between meteorology and soil radon confirms the link between the upper lithospheric air and the atmosphere, which moves due to convective, diffusion and other forces [51,52]. Earlier it was stated that the depth of 0.5–1 m is sufficient to exclude the influence of meteorological factors on soil radon [53], but there are a number of studies that contradict this fact [54–56]. The difference in temperature results in the release of radon into the atmosphere, and this effect increases with temperature. Since the daily activity layer affects the upper soil horizon, the effect on the daily change in soil radon content tends to decrease significantly with depth. Nevertheless, a significant seasonal difference in radon content is observed. Therefore, it is hypothesized that deep wells will reflect more of the seasonal cycle and shallow wells will reflect more of the diurnal variation. In permeable zones, this thermobaric effect is usually enhanced by the high permeability of the zone [23,57]. It is worth noting that the decrease in soil radon in the upper horizon may be associated with very high soil porosity. This territory is an agricultural field in which the top layer is quite well loosened. This circumstance has a beneficial effect on the exhalation of radon from the soil as a result of the temperature difference between the atmosphere and the soil.

4.2. RFD

Overall, across the entire study region, the RFD exhibits a moderately elevated level, which is relatively high for this type of area. Previously, we obtained significantly lower RFD values for a similar area, but without large faults, which were 22.87 $\pm$ 1 mBq·m^{-2}·s^{-1} at a distance of 0.8–1 km from the fault zone [58]. However, RFD increased significantly up

to 181.59 ± 13.32 mBq·m^{-2}·s^{-1} in areas where there were both disturbances and mine fields. The East Kamyshansky fault exhibited RFD values of up to 3310 mBq·m^{-2}·s^{-1}. At a distance of 350–400 m from the Vorobyovka fault offset, the RFD averaged 46.61 ± 3.62 mBq·m^{-2}·s^{-1}, with peak values reaching 260 mBq·m^{-2}·s^{-1}. Therefore, it can be assumed that the Zhurinskiy fault may presently be active, but this will require further investigation.

The lack of correlation between the distance from the observation point to the Zhurinsky fault displacement and the RFD can be explained by this distance apparently being insufficient to detect any influence of the fault on soil radon content. The difference in RFD is probably due to local characteristics (composition of loose sediments, radium content, etc.).

We did not find a relationship between soil VAR and RFD. Similar results have been obtained before [59]. For a similar area with loess-like loams, the authors also noted significant differences in RFD and soil radon [60]. Thus, high or low soil radon content may not be expressed in the increase in RFD. Apparently, the relationship between radon emanation to the surface, which is expressed in RFD, is lost with depth. Since the main causes of changes in RFD are the diurnal variation of temperature, the porosity of the sediments and moisture content, RFD alone may not be a reliable indicator for evaluating the safety of an area in terms of radon emissions.

For example, in clay soils the RFD will be significantly reduced, and soil radon can be dangerous. Thus, in the study of underground or deep structures, even in clay soils, radon had a high value [61]. There is reason to believe that a low RFD leads to an increase in soil radon due to a decrease in the rate of its discharge into the atmosphere due to the temperature difference between the lithosphere and the atmosphere. Therefore, soil radon assessment plays a crucial role, particularly in areas where there are plans to construct houses with basement levels.

We found a correlation between meteorology (air temperature, air, air humidity) and the moment of exposure of the storage chambers. Therefore, this soil layer is notably impacted by fluctuating levels of pressure, humidity and particularly air temperature which leads to a pressure difference between the lithosphere and the atmosphere and forms the soil air flow into the atmosphere [37,38].

In general, there is an increase in radon concentration with depth and its greater constancy during the day or season. Therefore, deeper soil horizons are more suitable for the study of soil radon. At the same time, the possibility of using these parameters for predicting radon emanation to the surface and, consequently, the informative value of the data in terms of safety for the population is reduced [62].

Air humidity affects the rate of water evaporation from the soil, especially in autumn when dew falls after sunset and before morning and the top layer of soil is heavily saturated. This excess moisture fills some pores, decreasing the space for radon diffusion. Low humidity in the atmosphere after sunrise leads to rapid evaporation of moisture from the soil, and high humidity and vice versa. Thus, measurements are taken in conditions with pores that are partially filled with moisture, resulting in a decreased RFD into the atmosphere. Comparable outcomes have been obtained in previous studies [63].

4.3. Spatial Patterns of RFD and Soil Air VAR

Based on the findings of Section 3.3, it can be inferred that the RFD is likely to exhibit lower values within the displacement zone as a result of the prevalence of compressive forces in that area. Conversely, the RFD may increase at a distance from the displacement zone due to the stretching of crustal blocks.

According to the presented figure, we can see some increase in RFD and in some cases and increase in soil air VAR in the hanging wall of the Zhurinsky fault. The hanging wall's permeability in the investigated disturbance zone has increased, which results in a significant increase in soil radon and indicates a significant radon hazard.

Linear, spot and "halo" anomalies of soil gas contents have been obtained in earlier studies [64]. It was also noted that high values should not be observed over the entire rock

crushing zone, in which case the local geological situation plays a role [65]. The formation of a patchy, discrete and highly permeable zone of deep gas emission was previously indicated. The main reasons for this form of gas anomalies have been identified as the evolution of the fault (its activity), fault style (its dynamic type (thrusting, faulting, fault rupture, etc.)), and the rheology of the rocks ruptured by the fault [66,67]. It is noted that with the increasing thickness of young sediments, faults have less influence on soil gas and RFD [64,68].

Previously, a study was conducted to identify neotectonic blocks in the Kuznetsk coal basin by analyzing data from vertex surfaces (watersheds) [69]. According to this work, the Zhurinsky fault is located on the boundary of neotectonic blocks which may indicate its activation. This process is usually accompanied by the creation of transport channels for deep gases (^{222}Rn, CH_4, CO_2, He, H_2, etc.).

Undoubtedly, the values of the VAR and RFD data were affected by the lack of data on the parent elements (Ra, U) in the soil, since their content can significantly increase soil radon and its emanation to the surface [70]. The predominance of the clay fraction in some observation points may lead to the growth of adsorbed uranium and radium in its particles. Fault zones may also act as collectors for uranium and radium in the process of their migration with groundwater [71,72].

It should not be excluded that this disturbance activity could be increased by active mining, causing changes in the stress–strain state of rocks. Concentrations of soil radon in this case will also change over time. Even a small change in the stress–strain state leads to a change in the radon field in the geological environment [73].

5. Conclusions

We evaluated the radon content in the soil and its emanation to the surface; no correlation was found between these indicators because with depth, the connection with daily meteorological parameters is lost. Strong correlations were found between RFD and meteorological parameters such as temperature, pressure, and humidity. This emphasizes the importance of considering these results in the permeable rock zone, which may include fault zones in the Earth's crust. The disturbance zone, which is frequently the limit of coal deposits, can also have a significant radiological impact. Convection–diffusion facilitates radon flow in this area.

The high radon concentration in this area poses a radiological hazard to the population when constructing residential buildings. Radon emanation is also a significant factor that must be considered when designing ventilation systems and constructing homes. Rock permeability enhances the migration of gases through rocks, including migration from significant depths. After the evaluation of soil radon content and RFD, we should assume the danger of this tectonic disturbance in terms of residential exposure.

Currently, there are no long-term observations, monitoring and extensive preliminary studies of the radon hazard of soils near the disturbance zone in the Kuznetsk coal basin. The preliminary results obtained from our study should be used to develop interim recommendations for the public to reduce radon exposure until radon hazardous areas are identified. The priority in the protection of homes is the forced ventilation of underground rooms or their separation from residential areas. In the future, a key need for these regions is the creation of a monitoring network aimed at assessing the characteristics of the radon field in fault zones.

Regarding further research, it is necessary to investigate the radon fields of other faults in Kuzbass, syngenetic to the Zhurinsky fault. It would also be an important addition to conduct a study of the content of ^{226}Ra in the studied soils and other deep gases (H_2, CH_4).

Author Contributions: Conceptualization, T.L. and A.L.; methodology, T.L.; software, T.L.; validation, K.L., T.L. and A.L.; formal analysis, T.L. and A.L.; investigation, K.L., T.L. and A.L.; resources, T.L. and A.L.; data curation, T.L.; writing—original draft preparation, T.L. and A.L.; writing—review and editing, K.L., T.L. and A.L.; visualization, T.L.; supervision, T.L.; project administration, A.L.; funding acquisition, A.L. All authors have read and agreed to the published version of the manuscript.

Funding: This research was funded by the Russian Science Foundation (RSF), under research project N° 23-27-00320, https://rscf.ru/en/project/23-27-00320/ (accessed on 22 October 2023).

Institutional Review Board Statement: Not applicable.

Informed Consent Statement: Not applicable.

Data Availability Statement: The data presented in this study are available in article.

Conflicts of Interest: The authors declare no conflict of interest.

References

1. Baeza, A.; García-Paniagua, J.; Guillén, J.; Montalbán, B. Influence of Architectural Style on Indoor Radon Concentration in a Radon Prone Area: A Case Study. *Sci. Total Environ.* **2018**, *610–611*, 258–266. [CrossRef] [PubMed]
2. Tsvetkova, T.; Przylibski, T.A.; Nevinsky, I.; Nevinsky, V. Measurement of Radon in the East Europe under the Ground. *Radiat. Meas.* **2005**, *40*, 98–105. [CrossRef]
3. Martin-Gisbert, L.; Ruano-Ravina, A.; Varela-Lema, L.; Penabad, M.; Giraldo-Osorio, A.; Candal-Pedreira, C.; Rey-Brandariz, J.; Mourino, N.; Pérez-Ríos, M. Lung Cancer Mortality Attributable to Residential Radon: A Systematic Scoping Review. *J. Expo. Sci. Environ. Epidemiol.* **2023**, *33*, 368–376. [CrossRef] [PubMed]
4. Lubin, J.H.; Boice, J.D. Lung Cancer Risk from Residential Radon: Meta-Analysis of Eight Epidemiologic Studies. *J. Natl. Cancer Inst.* **1997**, *89*, 49–57. [CrossRef] [PubMed]
5. Eidemüller, M.; Jacob, P.; Lane, R.S.D.; Frost, S.E.; Zablotska, L.B. Lung Cancer Mortality (1950–1999) among Eldorado Uranium Workers: A Comparison of Models of Carcinogenesis and Empirical Excess Risk Models. *PLoS ONE* **2012**, *7*, e41431. [CrossRef] [PubMed]
6. Noh, J.; Sohn, J.; Cho, J.; Kang, D.R.; Joo, S.; Kim, C.; Shin, D.C. Residential Radon and Environmental Burden of Disease among Non-Smokers. *Ann. Occup. Environ. Med.* **2016**, *28*, 12. [CrossRef] [PubMed]
7. Ajrouche, R.; Ielsch, G.; Cléro, E.; Roudier, C.; Gay, D.; Guillevic, J.; Laurier, D.; Le Tertre, A. Quantitative Health Risk Assessment of Indoor Radon: A Systematic Review. *Radiat. Prot. Dosim.* **2017**, *177*, 69–77. [CrossRef]
8. Malinovsky, G.; Yarmoshenko, I.; Zhukovsky, M. Radon, Smoking and HPV as Lung Cancer Risk Factors in Ecological Studies. *Int. J. Radiat. Biol.* **2018**, *94*, 62–69. [CrossRef]
9. Ma, Y.; Bringemeier, D.; Scheuermann, A.; Molebatsi, T.; Li, L. Fault and fracture zone detection based on soil gas mapping and gamma ray survey at the extension site of an open pit coal mine. In Proceedings of the 12th Coal Operators' Conference, University of Wollongong & The Australasian Institute of Mining and Metallurgy, Wollongong, Australia, 10–12 February 2012.
10. Giustini, F.; Ruggiero, L.; Sciarra, A.; Beaubien, S.E.; Graziani, S.; Galli, G.; Pizzino, L.; Tartarello, M.C.; Lucchetti, C.; Sirianni, P.; et al. Radon Hazard in Central Italy: Comparison among Areas with Different Geogenic Radon Potential. *Int. J. Environ. Res. Public Health* **2022**, *19*, 666. [CrossRef]
11. Wang, N.; Yang, J.; Wang, H.; Jia, B.; Peng, A. Characteristics of Indoor and Soil Gas Radon, and Discussion on High Radon Potential in Urumqi, Xinjiang, NW China. *Atmosphere* **2023**, *14*, 1548. [CrossRef]
12. Borgoni, R.; Tritto, V.; Bigliotto, C.; De Bartolo, D. A Geostatistical Approach to Assess the Spatial Association between Indoor Radon Concentration, Geological Features and Building Characteristics: The Case of Lombardy, Northern Italy. *Int. J. Environ. Res. Public Health* **2011**, *8*, 1420–1440. [CrossRef] [PubMed]
13. Gavriliev, S.; Petrova, T.; Miklyaev, P.; Karfidova, E. Predicting Radon Flux Density from Soil Surface Using Machine Learning and GIS Data. *Sci. Total Environ.* **2023**, *903*, 166348. [CrossRef]
14. Cinelli, G.; Tositti, L.; Capaccioni, B.; Brattich, E.; Mostacci, D. Soil Gas Radon Assessment and Development of a Radon Risk Map in Bolsena, Central Italy. *Environ. Geochem. Health* **2015**, *37*, 305–319. [CrossRef] [PubMed]
15. Kemski, J.; Klingel, R.; Siehl, A.; Valdivia-Manchego, M. From Radon Hazard to Risk Prediction-Based on Geological Maps, Soil Gas and Indoor Measurements in Germany. *Environ. Geol.* **2009**, *56*, 1269–1279. [CrossRef]
16. Moussa, M.M.; El Arabi, A.-G.M. Soil Radon Survey for Tracing Active Fault: A Case Study along Qena-Safaga Road, Eastern Desert, Egypt. *Radiat. Meas.* **2003**, *37*, 211–216. [CrossRef]
17. Utkin, V.I.; Yurkov, A.K. Radon as a Tracer of Tectonic Movements. *Russ. Geol. Geophys.* **2010**, *51*, 220–227. [CrossRef]
18. Voltattorni, N.; Sciarra, A.; Quattrocchi, F. The Application of Soil Gas Technique to Geothermal Exploration:Study of "Hidden" Potential Geothermal Systems. In Proceedings of the World Geothermal Congress 2010, Bali, Indonesia, 25–29 April 2010.
19. Ciotoli, G.; Bigi, S.; Tartarello, C.; Sacco, P.; Lombardi, S.; Ascione, A.; Mazzoli, S. Soil Gas Distribution in the Main Coseismic Surface Rupture Zone of the 1980, Ms = 6.9, Irpinia Earthquake (Southern Italy). *J. Geophys. Res. Solid Earth* **2014**, *119*, 2440–2461. [CrossRef]
20. Seminsky, K.Z.; Bobrov, A.A. Radon Activity of Faults (Western Baikal and Southern Angara Areas). *Russ. Geol. Geophys.* **2009**, *50*, 682–692. [CrossRef]
21. Seminsky, K.Z.; Bobrov, A.A.; Demberel, S. Variations in radon activity in the crustal fault zonez: Spatial characteristics. *Izvestiya Phys. Solid Earth* **2014**, *50*, 795–813. [CrossRef]
22. Pereira, A.J.S.C.; Godinho, M.M.; Neves, L.J.P.F. On the Influence of Faulting on Small-Scale Soil-Gas Radon Variability: A Case Study in the Iberian Uranium Province. *J. Environ. Radioact.* **2010**, *101*, 875–882. [CrossRef]

23. Miklyaev, P.S.; Petrova, T.B.; Shchitov, D.V.; Sidyakin, P.A.; Murzabekov, M.A.; Tsebro, D.N.; Marennyy, A.M.; Nefedov, N.A.; Gavriliev, S.G. Radon Transport in Permeable Geological Environments. *Sci. Total Environ.* **2022**, *852*, 158382. [CrossRef] [PubMed]
24. Steinitz, G.; Vulkan; Lang; Gilat, A.; Zafrir, H. Radon Emanation along Border Faults of the Rift in the Dead Sea Area. *Isr. J. Earth Sci.* **1992**, *41*, 9–20.
25. Kamra, L. Seasonal Emanation of Radon at Ghuttu, Northwest Himalaya: Differentiation of Atmospheric Temperature and Pressure Influences. *Appl. Radiat. Isot.* **2015**, *105*, 170–175. [CrossRef] [PubMed]
26. Chakraverty, S.; Sahoo, B.K.; Rao, T.D.; Karunakar, P.; Sapra, B.K. Modelling Uncertainties in the Diffusion-Advection Equation for Radon Transport in Soil Using Interval Arithmetic. *J. Environ. Radioact.* **2018**, *182*, 165–171. [CrossRef] [PubMed]
27. Toader, V.-E.; Mihai, A.; Moldovan, I.-A.; Ionescu, C.; Marmureanu, A.; Lingvay, I. Implementation of a Radon Monitoring Network in a Seismic Area. *Atmosphere* **2021**, *12*, 1041. [CrossRef]
28. Zaalishvili, V.; Melkov, D.; Revazov, M. Relationship of radon emanation with the level of external impact according to large landslides monitoring in mountain areas. *Sustain. Dev. Mt. Territ.* **2021**, *13*, 564–575. [CrossRef]
29. Leshukov, T.; Larionov, A.; Legoshchin, K.; Yakovleva, S. Radon Hazard Assessment in Region with Intense Coal Mining Industry. *IOP Conf. Ser. Earth Environ. Sci.* **2020**, *543*, 012026. [CrossRef]
30. Leshukov, T.; Larionov, A.; Legoshchin, K.; Lesin, Y.; Yakovleva, S. The Assessment of Radon Emissions as Results of the Soil Technogenic Disturbance. *Int. J. Environ. Res. Public Health* **2020**, *17*, 9268. [CrossRef]
31. Ball, T.K.; Wysocka, M. Radon in Coalfields in the United Kingdom and Poland. *Arch. Min. Sci.* **2011**, *56*, 249–264.
32. Klingel, R.; Kemski, J. *Influence of Underground Mining on the Geogenic Radon Potential*; Radon Living Environment: Athens, Greece, 1999; pp. 773–786.
33. Lu, W.; Cao, Y.-J.; Tien, J. Method for Prevention and Control of Spontaneous Combustion of Coal Seam and Its Application in Mining Field. *Int. J. Min. Sci. Technol.* **2017**, *27*, 839–846. [CrossRef]
34. Palchik, V. Localization of Mining-Induced Horizontal Fractures along Rock Layer Interfaces in Overburden: Field Measurements and Prediction. *Environ. Geol.* **2005**, *48*, 68–80. [CrossRef]
35. Wysocka, M.; Chalupnik, S. Correlation of Radon Concentration Level with Mining and Geological Conditions in Upper Silesia Region. *J. Min. Sci.* **2003**, *2*, 199–206. [CrossRef]
36. Wysocka, M.; Nowak, S.; Chałupnik, S.; Bonczyk, M. Radon Concentrations in Dwellings in the Mining Area—Are There Observed Effects of the Coal Mine Closure? *Int. J. Environ. Res. Public Health* **2022**, *19*, 5214. [CrossRef] [PubMed]
37. Schery, S.D.; Gaeddert, D.H. Measurements of the Effect of Cyclic Atmospheric Pressure Variation on the Flux of 222RN from the Soil. *Geophys. Res. Lett.* **1982**, *9*, 835–838. [CrossRef]
38. Modibo, O.B.; Tamakuma, Y.; Suzuki, T.; Yamada, R.; Zhuo, W.; Kranrod, C.; Iwaoka, K.; Akata, N.; Hosoda, M.; Tokonami, S. Long-Term Measurements of Radon and Thoron Exhalation Rates from the Ground Using the Vertical Distributions of Their Activity Concentrations. *Int. J. Environ. Res. Public Health* **2021**, *18*, 1489. [CrossRef] [PubMed]
39. Bichkov, A.I.; Shatilova, G.I.; Shigrev, A.F. *Geological Structure and Minerals of the Central Part of Kuzbass*; Report of the Kuzbass Party on the Compilation of a Geological Map and a Map of Mineral Resources at a Scale of 1:50000 on the Gramoteinskaya Area within the Framework of Sheets No. 45-41-B, D and No. 45-53-A, B, C, G.; KPR Kemerovskoy Oblasti: Novokuznetsk, Russia, 1998.
40. Lavrenov, P.F.; Snegko, B.A.; Shigrev, A.F.; Shelemeteva, A.V.; Filippova, N.V. *State Geological Map of the Russian Federation. Scale 1: 200,000*, 2nd ed.; Kuzbass Series, Sheet N-45-XV (Leninsk-Kuznetsky), Explanatory Letter; VSEGEI: Moscow, Russia, 2018.
41. Maier, A.; Jones, J.; Sternkopf, S.; Friedrich, E.; Fournier, C.; Kraft, G. Radon Adsorption in Charcoal. *Int. J. Environ. Res. Public Health* **2021**, *18*, 4454. [CrossRef]
42. *NRB99/2009*; Radiation Safety Standards: Sanitary and Epidemiological Rules and Regulations. Federal Center for Hygiene and Epidemiology of Rospotrebnadzor: Moscow, Russia, 2009.
43. Neri, M.; Giammanco, S.; Leonardi, A. Preliminary Indoor Radon Measurements near Faults Crossing Urban Areas of Mt. Etna Volcano (Italy). *Front. Public Health* **2019**, *7*, 105. [CrossRef] [PubMed]
44. Etiope, G.; Lombardi, S. Evidence for Radon Transport by Carrier Gas through Faulted Clays in Italy. *J. Radioanal. Nucl. Chem.* **1995**, *193*, 291–300. [CrossRef]
45. Cvetković, M.; Kapuralić, J.; Pejić, M.; Kolenković Močilac, I.; Rukavina, D.; Smirčić, D.; Kamenski, A.; Matoš, B.; Špelić, M. Soil Gas Measurements of Radon, CO_2 and Hydrocarbon Concentrations as Indicators of Subsurface Hydrocarbon Accumulation and Hydrocarbon Seepage. *Sustainability* **2021**, *13*, 3840. [CrossRef]
46. Dyck, W.; Jonasson, I.R. Chapter 11 Radon. In *Handbook of Exploration Geochemistry*; Hale, M., Ed.; Geochemical Remote Sensing of the Sub-Surface; Elsevier Science B.V.: Amsterdam, The Netherlands, 2000; Volume 7, pp. 353–394.
47. Okeme, I.C.; Scott, T.B.; Martin, P.G.; Satou, Y.; Ojonimi, T.I.; Olaluwoye, M.O. Assessment of the Mode of Occurrence and Radiological Impact of Radionuclides in Nigerian Coal and Resultant Post-Combustion Coal Ash Using Scanning Electron Microscopy and Gamma-Ray Spectroscopy. *Minerals* **2020**, *10*, 241. [CrossRef]
48. Benà, E.; Ciotoli, G.; Ruggiero, L.; Coletti, C.; Bossew, P.; Massironi, M.; Mazzoli, C.; Mair, V.; Morelli, C.; Galgaro, A.; et al. Evaluation of Tectonically Enhanced Radon in Fault Zones by Quantification of the Radon Activity Index. *Sci. Rep.* **2022**, *12*, 21586. [CrossRef] [PubMed]

49. Lara, E.; Rocha, Z.; Palmieri, H.E.L.; Santos, T.O.; Rios, F.J.; Oliveira, A.H. Radon Concentration in Soil Gas and Its Correlations with Pedologies, Permeabilities and 226Ra Content in the Soil of the Metropolitan Region of Belo Horizonte—RMBH, Brazil. *Radiat. Phys. Chem.* **2015**, *116*, 317–320. [CrossRef]
50. Nunes, L.J.R.; Curado, A.; Lopes, S.I. The Relationship between Radon and Geology: Sources, Transport and Indoor Accumulation. *Appl. Sci.* **2023**, *13*, 7460. [CrossRef]
51. Smetanová, I.; Holý, K.; Müllerová, M.; Polášková, A. The Effect of Meteorological Parameters on Radon Concentration in Borehole Air and Water. *J. Radioanal. Nucl. Chem.* **2010**, *283*, 101–109. [CrossRef]
52. Hinkle, M.E. Environmental Conditions Affecting Concentrations of He, CO_2, O_2 and N_2 in Soil Gases. *Appl. Geochem.* **1994**, *9*, 53–63. [CrossRef]
53. Kemski, J.; Siehl, A.; Stegemann, R.; Valdivia-Manchego, M. Mapping the Geogenic Radon Potential in Germany. *Sci. Total Environ.* **2001**, *272*, 217–230. [CrossRef] [PubMed]
54. Haquin, G.; Zafrir, H.; Ilzycer, D.; Weisbrod, N. Effect of Atmospheric Temperature on Underground Radon: A Laboratory Experiment. *J. Environ. Radioact.* **2022**, *253–254*, 106992. [CrossRef]
55. Catalano, R.; Immé, G.; Mangano, G.; Morelli, D.; Aranzulla, M. Radon Transport: Laboratory and Model Study. *Radiat. Prot. Dosim.* **2015**, *164*, 575–581. [CrossRef]
56. Siino, M.; Scudero, S.; Cannelli, V.; Piersanti, A.; D'Alessandro, A. Multiple Seasonality in Soil Radon Time Series. *Sci. Rep.* **2019**, *9*, 8610. [CrossRef]
57. Benkovitz, A.; Zafrir, H.; Reuveni, Y. A Novel Assessment of the Surface Heat Flux Role in Radon (Rn-222) Gas Flow within Subsurface Geological Porous Media. *Remote Sens.* **2023**, *15*, 4094. [CrossRef]
58. Leshukov, T. Radon Hazard in Underground Coal Mining Areas (Using the Example of the Kuznetsk Coal Basin). Candidate's Thesis, KemSU, Grozny, Russia, 2021.
59. Rábago, D.; Quindós, L.; Vargas, A.; Sainz, C.; Radulescu, I.; Ioan, M.-R.; Cardellini, F.; Capogni, M.; Rizzo, A.; Celaya, S.; et al. Intercomparison of Radon Flux Monitors at Low and at High Radium Content Areas under Field Conditions. *Int. J. Environ. Res. Public Health* **2022**, *19*, 4213. [CrossRef] [PubMed]
60. Ryzhakova, N.K.; Stavitskaya, K.O.; Plastun, S.A. The Problems of Assessing Radon Hazard of Development Sites in the Russian Federation and the Czech Republic. *Radiat. Meas.* **2022**, *150*, 106681. [CrossRef]
61. Rizo Maestre, C.; Echarri Iribarren, V. The Radon Gas in Underground Buildings in Clay Soils. The Plaza Balmis Shelter as a Paradigm. *Int. J. Environ. Res. Public Health* **2018**, *15*, 1004. [CrossRef] [PubMed]
62. Mao, Y.; Zhang, L.; Wang, H.; Guo, Q. The Temporal Variation of Radon Concentration at Different Depths of Soil: A Case Study in Beijing. *J. Environ. Radioact.* **2023**, *264*, 107200. [CrossRef] [PubMed]
63. Shweikani, R.; Giaddui, T.G.; Durrani, S.A. The Effect of Soil Parameters on the Radon Concentration Values in the Environment. *Radiat. Meas.* **1995**, *25*, 581–584. [CrossRef]
64. Ciotoli, G.; Lombardi, S.; Annunziatellis, A. Geostatistical Analysis of Soil Gas Data in a High Seismic Intermontane Basin: Fucino Plain, Central Italy. *J. Geophys. Res. Solid Earth* **2007**, *112*, JB004044. [CrossRef]
65. Ciotoli, G.; Lombardi, S.; Zarlenga, F. Natural leakage of helium from Italian sedimentary basins of the Adriatic structural margin. In *Advances in the Geological Storage of Carbon Dioxide*; Lombardi, S., Altunina, L.K., Beaubien, S.E., Eds.; Springer: Dordrecht, The Netherlands, 2006; pp. 191–202.
66. Annunziatellis, A.; Beaubien, S.E.; Bigi, S.; Ciotoli, G.; Coltella, M.; Lombardi, S. Gas Migration along Fault Systems and through the Vadose Zone in the Latera Caldera (Central Italy): Implications for CO_2 Geological Storage. *Int. J. Greenh. Gas Control* **2008**, *2*, 353–372. [CrossRef]
67. Seminskii, K.; Bobrov, A.A.; Sodnomsambuu, D. Relationship between Radon and the Tectonic Activity of Faults in Central Mongolia. *Dokl. Earth Sci.* **2019**, *487*, 890–893. [CrossRef]
68. Berberich, G.M.; Berberich, M.B. Comparison of Geogases in Two Cenozoic Sedimentary Basins. *Geosciences* **2022**, *12*, 388. [CrossRef]
69. Novikov, I.S.; Cherkas, O.V.; Mamedov, G.M.; Simonov, Y.G.; Simonova, T.Y.; Nastavko, V.G. Activity stages and tectonic division in the Kuznetsk Basin, Southern Siberia. *Russ. Geol. Geophys.* **2013**, *54*, 324–334. [CrossRef]
70. Pereira, A.; Lamas, R.; Miranda, M.; Domingos, F.; Neves, L.; Ferreira, N.; Costa, L. Estimation of the Radon Production Rate in Granite Rocks and Evaluation of the Implications for Geogenic Radon Potential Maps: A Case Study in Central Portugal. *J. Environ. Radioact.* **2017**, *166*, 270–277. [CrossRef] [PubMed]
71. Pereira, A.J.S.C.; Neves, L.J.P.F. Estimation of the Radiological Background and Dose Assessment in Areas with Naturally Occurring Uranium Geochemical Anomalies—A Case Study in the Iberian Massif (Central Portugal). *J. Environ. Radioact.* **2012**, *112*, 96–107. [CrossRef] [PubMed]

72. Cho, S.Y.; Koo, M.-H.; Cho, B.W.; Jung, Y.-Y.; Oh, Y.H. Factors Controlling the Spatial and Temporal Variability in Groundwater 222Rn and U Levels. *Water* **2019**, *11*, 1796. [CrossRef]
73. Galiana-Merino, J.J.; Molina, S.; Kharazian, A.; Toader, V.-E.; Moldovan, I.-A.; Gómez, I. Analysis of Radon Measurements in Relation to Daily Seismic Activity Rates in the Vrancea Region, Romania. *Sensors* **2022**, *22*, 4160. [CrossRef]

Disclaimer/Publisher's Note: The statements, opinions and data contained in all publications are solely those of the individual author(s) and contributor(s) and not of MDPI and/or the editor(s). MDPI and/or the editor(s) disclaim responsibility for any injury to people or property resulting from any ideas, methods, instructions or products referred to in the content.